AD-A136 108   A REFINED MODEL FOR RADAR HOMING INTERCEPTS(U)   1/1
               MASSACHUSETTS INST OF TECH LEXINGTON LINCOLN LAB
               M J TSAI ET AL. 27 OCT 83 TR-657 ESD-TR-83-045
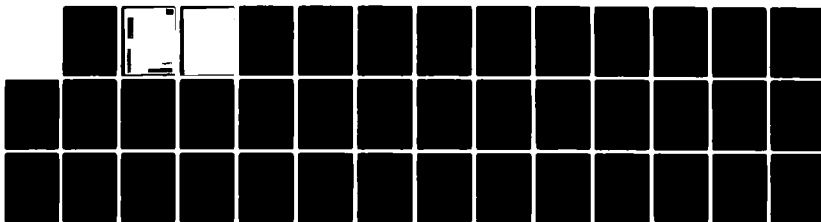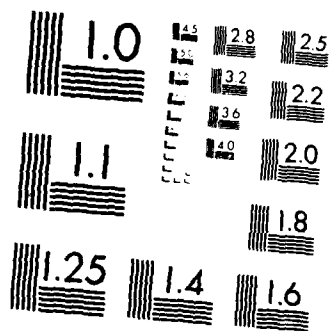UNCLASSIFIED   F19628-80-C-0002   F/G 17/7   NL

END
DATE
FILMED
1-84
DTIC

MICROCOPY RESOLUTION TEST CHART

NATIONAL BUREAU OF STANDARDS-1963-A

AD-A136 108

Technical Report
657

A Refined Model for Radar Homing Intercepts

M.J. Tsai
S.D. Weiner

27 October 1983

Lincoln Laboratory

MASSACHUSETTS INSTITUTE OF TECHNOLOGY

LEXINGTON, MASSACHUSETTS

DTIC

DEC 21 1983

A

83 12 20 116

This technical report has been reviewed and is approved for publication.

FOR THE COMMANDER

Thomas J. Alpert, Major, USAF
Chief, ESD Lincoln Laboratory Project Office

MASSACHUSETTS INSTITUTE OF TECHNOLOGY
LINCOLN LABORATORY

A REFINED MODEL FOR RADAR
HOMING INTERCEPTS

M.J. TSAI
S.D. WEINER

Group 32

TECHNICAL REPORT 657

27 OCTOBER 1983

LEXINGTON   MASSACHUSETTS

ABSTRACT

In this report, we extend a simple graphical model for analyzing radar homing interceptor engagements [1] to include the radome refraction error effect and a refined miss distance estimator. The residual radome error is treated as an additive exponentially correlated noise with correlation time equal to the interceptor response time. The miss distance is estimated as the error in predicting the target cross-range position at intercept at the range where the interceptor divert capability becomes just insufficient to correct the distance difference between the previous and the current predicted intercept points. The analytical and numerical results show that the prediction error is a strong function of the correlation time and the effect of correlation generally increases the achievable miss distance especially when the interceptor response time is large.

iii

CONTENTS

I.   INTRODUCTION

There is considerable interest in evaluating the performance of homing interceptors using simple analysis techniques [1, 2]. The analytical results are generally good enough for system-level studies and could be used as guides for complicated computer simulations.

In [1], a simple graphical model for analyzing radar homing interceptor engagements was presented. The model compares the accuracy of the intercept point prediction and the interceptor divert capability to estimate the final miss distance. At long ranges, the interceptor can usually take out the prediction error because of the long time remaining until intercept. However, at sufficient close ranges, the interceptor is no longer capable of fully correcting the prediction error and this residual error is considered as a rough estimate of the miss distance. In this model, the sensor error is treated as a white noise and it is assumed that the interceptor responds to the sensor prediction perfectly. (This has been called "divine guidance.")

In this report, we extend the previous model [1] to include the boresight slope error effect and a refined engagement model. The boresight slope error which is believed to be important to the final miss distance is modeled as a correlated noise additive

to the measurement [3, 4]. The analytical and numerical results show that the prediction error is a strong function of the correlation time of the noise. Besides, the effects of correlation generally increase the achievable miss distance, especially when the interceptor response time is large.

The refined engagement model assumes that the sensor revises the prediction of target position at intercept at each pulse and the interceptor changes maneuver accordingly to get to the predicted position. The miss distance is then regarded as the prediction error at the range where the interceptor divert capability becomes insufficient to correct the distance difference between the previous and the current predicted target positions.

In the next section, we first summarize the basic model described in [1] in order to provide a foundation for the following discussions. In Section 3, we describe the refined sensor error model and the resulting prediction errors. Section 4 describes the final miss distance model and presents some numerical results. Finally, a conclusion is given. There are two appendices containing detailed derivations of the statistical formula used in Sections 3 and 4.

II. BASIC MODEL

In this section, we summarize the basic sensor; interceptor and engagement models are presented in [1]. The homing sensor tracks a target from acquisition range r_a to a given range r and predicts ahead to intercept (range=0). Based on a sequence of measurements of the target cross-range position, z_i (i=1,..., N), at range r_i with accuracy σ_i and assuming a linear target trajectory model

$$z_i = \beta_0 + \beta_1 r_i + w_i \tag{1}$$

where w_i i=1,..., N is a sequence of uncorrelated zero-mean noise, the general formula for the predicted position ($\hat{\beta}_0$) and the prediction error $\sigma(\hat{\beta}_0) = \sqrt{\text{Var}(\hat{\beta}_0)}$ have been derived. Among various radar error sources, we are particularly concerned with the instrumentation error. For this error, $\sigma_i = \sigma_\theta r_i$ where σ_θ is the radar angular accuracy and β_0 and Var (β_0) are given by

$$\hat{\beta}_0 = \frac{\displaystyle\sum_{i=1}^{N} \frac{z_i}{r_i^2} - \frac{1}{N} \sum_{i=1}^{N} \frac{z_i}{r_i} \sum_{i=1}^{N} \frac{1}{r_i}}{\displaystyle\sum_{i=1}^{N} \frac{1}{r_i^2} - \frac{1}{N} \left(\sum_{i=1}^{N} \frac{1}{r_i} \right)^2} \tag{2}$$

and

$$Var(\hat{\beta}_0) = \frac{\sigma_\theta^2}{\sum\limits_{i=1}^{N} \frac{1}{r_i^2} - \frac{1}{N}\left(\sum\limits_{i=1}^{N} \frac{1}{r_i}\right)^2} \tag{3}$$

respectively.

The interceptor response to a commanded acceleration is modeled as a constant acceleration preceded by a pure time delay, τ_m. Thus, the divert capability of the interceptor at range r is equal to

$$D = 1/2\ a(r/v_c - \tau_m) \tag{4}$$

where v_c is the closing velocity and a is the maneuver acceleration limit.

During engagement, at an instantaneous range after acquisition at which tracking stops and prediction starts, the interceptor is commanded to erase the prediction error. In the early stage of engagement, the divert capability of the interceptor is usually more than enough to do so. However as r decreases, the divert capability decreases faster than the prediction error and so at some point the divert is just adequate to take out the prediction error. Below this point, the divert becomes insufficient. The corresponding prediction error at this point is then considered as an estimate of the final miss distance.

4

III. A BETTER SENSOR NOISE MODEL

In this section, we calculate the predicted target position
at intercept and the associated prediction error using a refined
sensor noise model which can take the radome refraction error
into account. We will follow the same notation as used in the
previous section.

It has been pointed out that the radome refraction error
could cause instability of the interceptor [3] and should be
compensated by an on-board computer using pre-calibrated look-up
tables. Even after compensation, the residual error is still
expected to influence the performance of the interceptor. This
residual radome error is modeled as an exponentially correlated
noise in the look angle domain [4]. By proper choice of error
magnitude and correlation distance, it is possible to match the
appropriate boresite slope error distribution. In simulation,
this correlated noise can be generated by passing a white
sequence through a first order Markov process filter.

We assume that noises additive to the target cross-range
position measurements due to radome refraction are also
exponentially correlated but in the range or time domain. That
is

$$E [w_i \, w_j] = \sigma_i \, \sigma_j \, \rho^{|j-i|} \tag{5a}$$

$$\rho = \exp\,(-\Delta t/\tau_c) = \exp\,(-1/(prf\cdot\tau_c)) \qquad (5b)$$

where Δt, equal to $1/prf$, is the pulse interval and τ_c is the correlation time. If the interceptor does not maneuver by changing its angle of attack, the $\tau_c \to \infty$. If the interceptor does maneuver, then a reasonable assumption for τ_c is that it is equal to the missile response time, τ_m. This is because the look angles are likely to be correlated within τ_m due to lack of maneuver change but tend to vary significantly over a period longer than τ_m due to the new maneuver.

According to this error model, it is shown in Appendix I that $\hat{\beta}_0$ and $\text{Var}(\hat{\beta}_0)$ are given by

$$\hat{\beta}_0 = \alpha\,\{f(\underline{r},\,\underline{r})\,f(\underline{z},\,\underline{j}) - f(\underline{r},\,\underline{z})\,f(\underline{r},\,\underline{j})\} \qquad (6)$$

$$\text{Var}(\hat{\beta}_0) = \sigma_\theta^2\,(1-\rho^2)\,\alpha\,f(\underline{r},\,\underline{r}) \qquad (7)$$

where

$$\alpha = \{f(\underline{j},\,\underline{j})\,f(\underline{r},\,\underline{r}) - f^2\,(\underline{r},\,\underline{j})\}^{-1}$$

$$f(\underline{u},\,\underline{v}) = \left\{\sum_{i=1}^{N-1} \left(\frac{u_i}{r_i} - \frac{\rho\,u_{i+1}}{r_{i+1}}\right)\left(\frac{v_i}{r_i} - \frac{\rho\,v_{i+1}}{r_{i+1}}\right)\right\} + (1-\rho^2)\,\frac{u_N\,v_N}{r_N^2}$$

$$\underline{j} = (1,\ldots,\,1),\quad \underline{r} = (r_1,\ldots,\,r_N),\quad \underline{z} = (z_1,\ldots,\,z_N)$$

6

when $\sigma_i = \sigma_\theta r_i$. Here σ_θ might represent the magnitude of the residual radome refraction error or the radar range-independent (instrumentation) error. To be more explicit, $\text{var}(\hat{\beta}_0)$ in (7) can be rewritten

$$\text{Var}(\hat{\beta}_0) = \frac{\sigma_\theta^2 (1 - \rho^2)}{\left\{ \sum_{i=1}^{N-1} \left(\frac{1}{r_i} - \frac{\rho}{r_{i+1}} \right)^2 + \frac{1-\rho^2}{r_N} \right\} - \left(N + \frac{2\rho}{1-\rho} \right)^{-1} \left\{ \sum_{i=1}^{N-1} \left(\frac{1}{r_i} - \frac{\rho}{r_{i+1}} \right) + \frac{1+\rho}{r_N} \right\}^2}$$

(7a)

Note that when $\rho=0$ (or $\tau_c=0$), the case of uncorrelated noise, the above two equations reduce to (2) and (3) as expected.

Figure 1 shows the prediction error as a function of the instantaneous range r for several values of τ_c using a set of nominal values for r_a(5 km), v_c(5 km/s), prf(100) and σ_θ(2 mr). It is clear that at long ranges the correlation degrades the prediction accuracy but starts to improve it near intercept. This behavior can be explained as follows: The effects of correlation are twofold. On one hand, higher correlation means fewer independent samples and so larger $\sigma(\hat{\beta}_0)$. On the other hand, with short time to intercept, the higher correlation imposes strong proportionality constraints among samples [5] and reduces the dependence of $\hat{\beta}_0$ on the noise. In the limiting case where $\rho=1$ (or $\tau_c=\infty$), for any given w_1, the subsequent noise samples are restricted to be
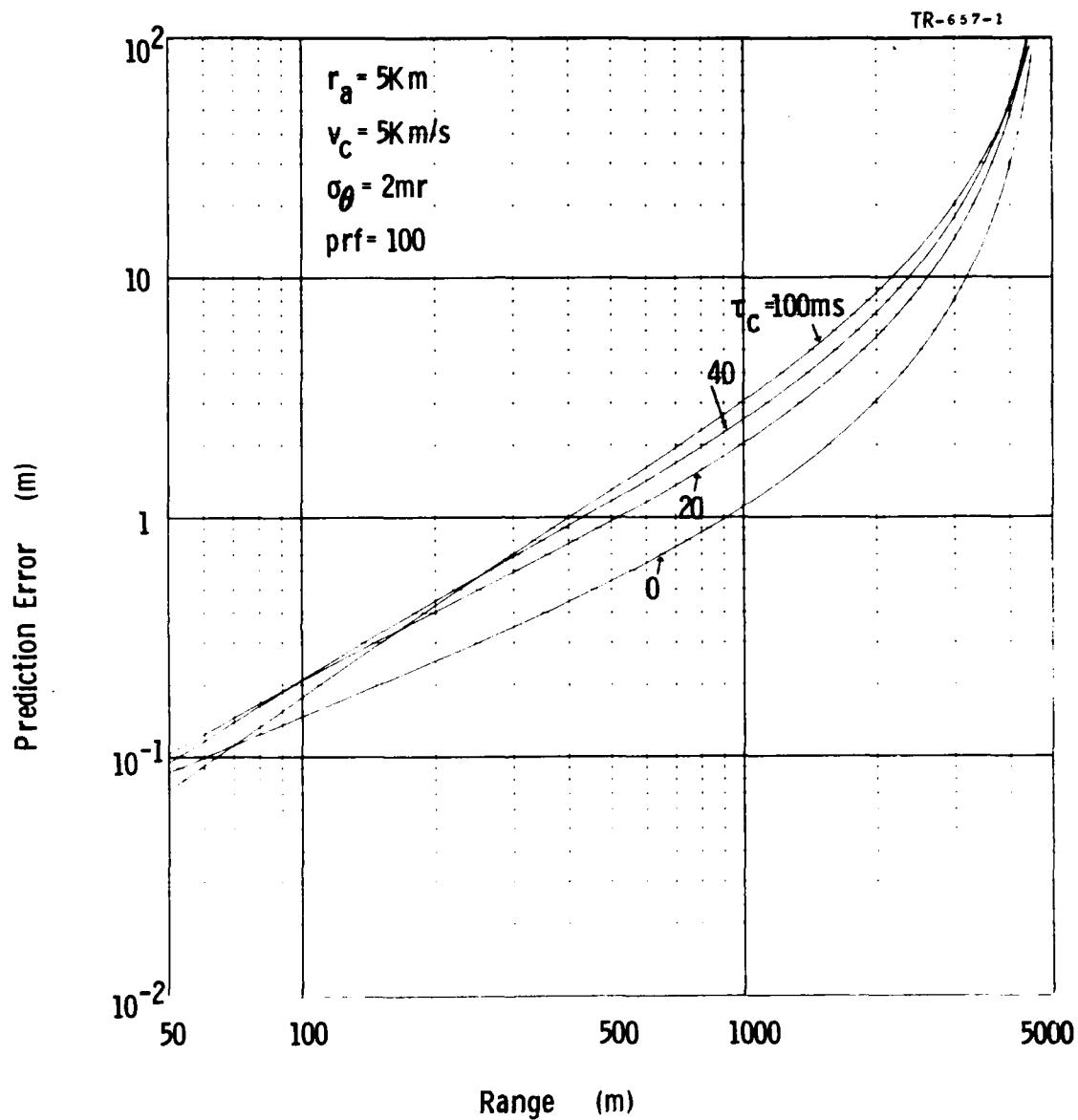
7

Fig. 1.   Prediction error - example 1.

8

$$w_i = \frac{\sigma_i}{\sigma_1} \quad w_1 \qquad \qquad i=2,..,N$$

and (1) can be written as

$$z_i = \beta_0 + (\beta_1 + \frac{w_1}{r_1}) \quad r_i$$

Clearly, the noise does not affect β_0 and therefore $\hat{\beta}_0$ is always equal to β_0 and $\sigma(\hat{\beta}_0)=0$. At long ranges, the number of available samples is small and so the first effect might dominate for moderate values of ρ. Near intercept, many samples become available. The first effect is less important and is overwhelmed by the second effect. In fact, it can be shown that for $r<<v_c/prf$,

$$\sigma(\hat{\beta}_0) = \sigma_\theta \quad r \quad \sqrt{1-\rho^2} \qquad . \qquad (8)$$

However, this corresponds to the region after the last measurement.

Figures 2 and 3, in comparison to Figure 1, show the effect of prf on the prediction error while σ_θ is kept constant. Generally speaking, higher prf tends to reduce the prediction error for the case $\tau_c = 0$ but not for the other cases.
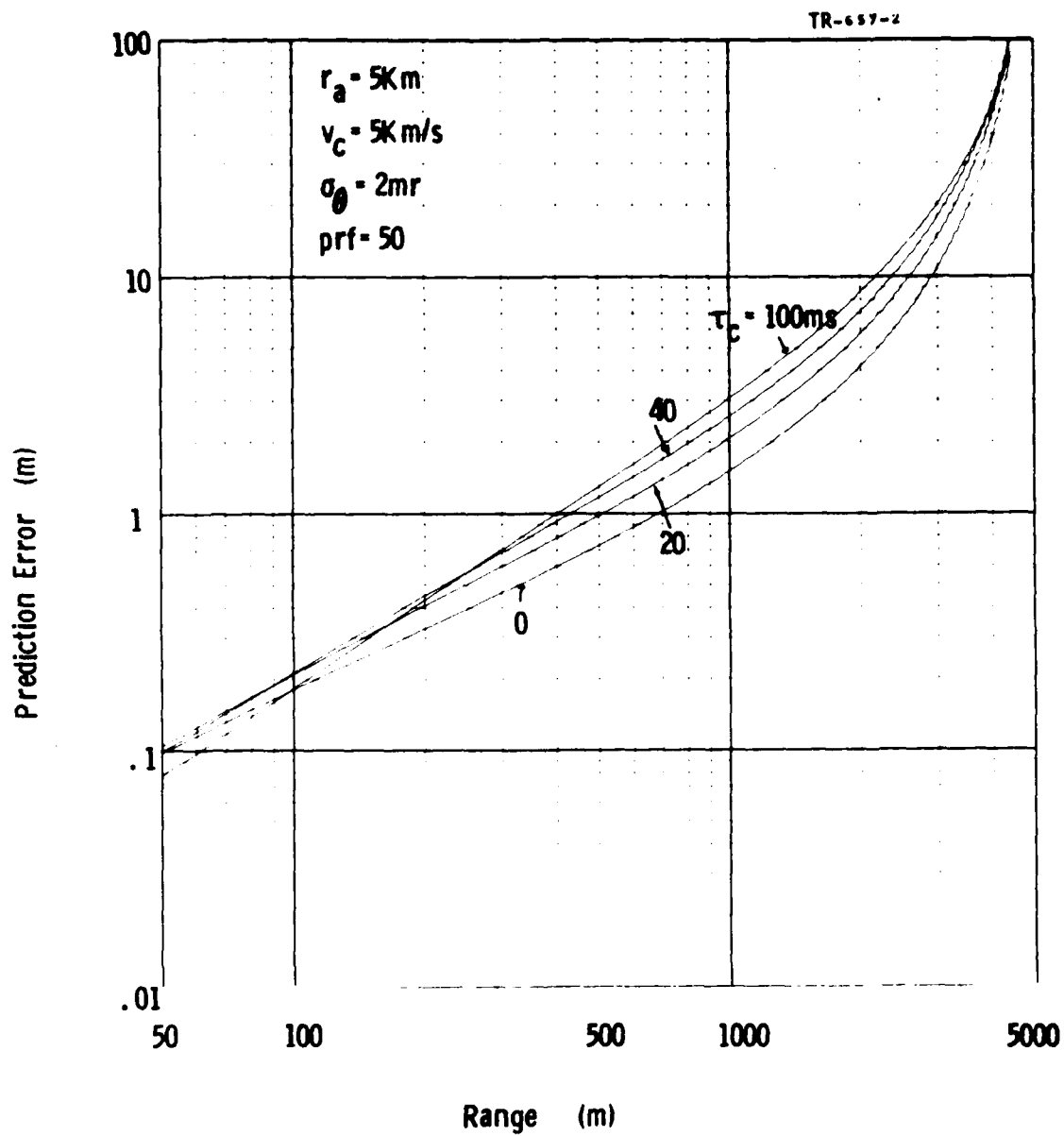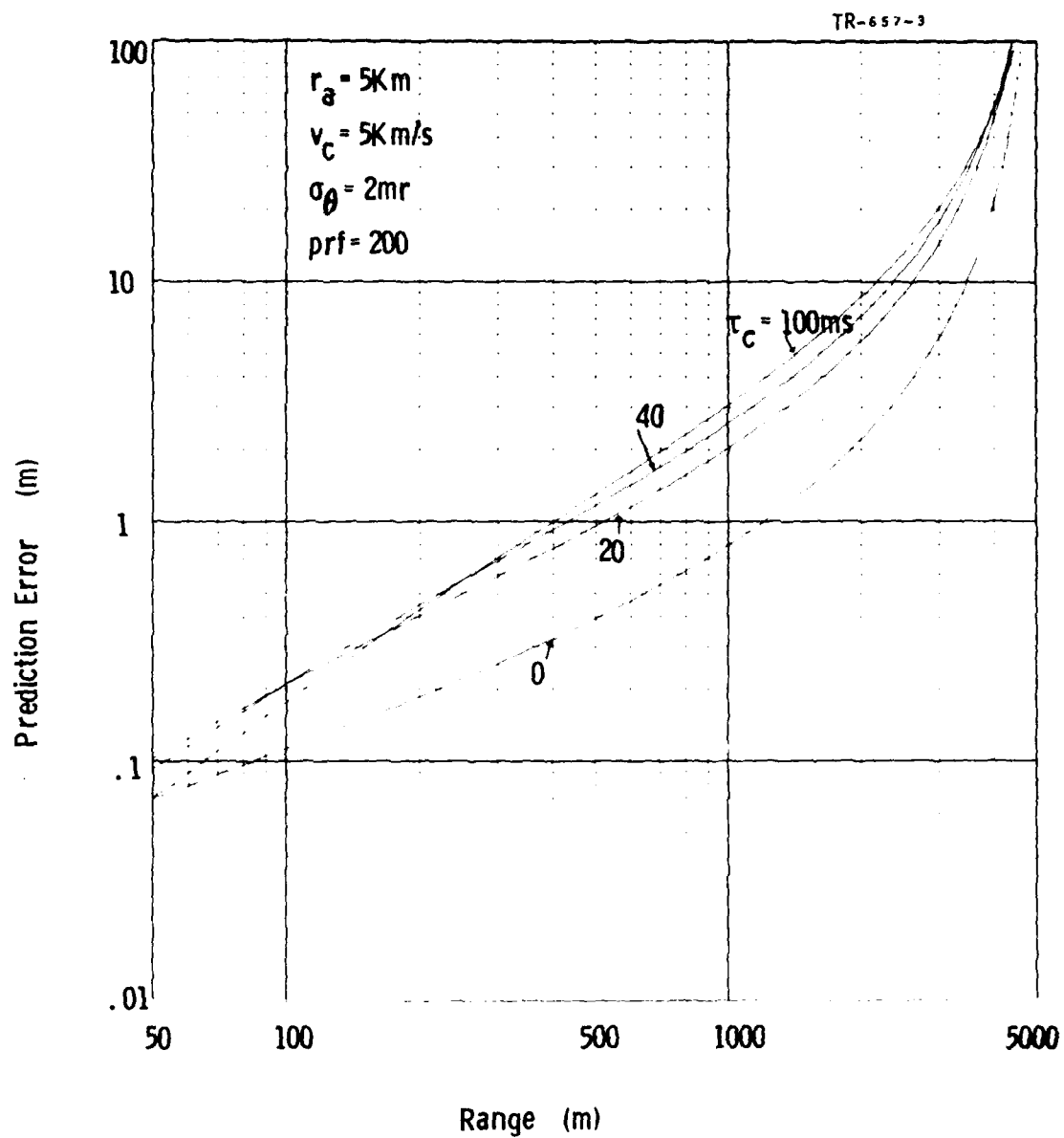
Fig. 2. Prediction error - example 2.

Fig. 3. Prediction error - example 3.

IV. MISS DISTANCE MODEL

The intercept point predicted by the homing sensor changes
from pulse to the pulse. At the Nth pulse, the interceptor
responds to the revised prediction by maneuvering to take out the
difference between $\hat{\beta}_0(N)$ and $\hat{\beta}_0(N-1)$ within the remaining time
until intercept. In other words, the interceptor is commanded to
chase the predicted intercept point. During the engagement
process, the instantaneous miss distance becomes smaller and
smaller as the interceptor approaches the target. At some point
the divert capability of the interceptor becomes insufficient to
respond to the change in predicted target position. At this
critical point, the prediction error can no longer be reduced and
it is considered as an estimate of the final miss distance.

The one-pulse position change at Nth pulse is a random
variable. Let $\Delta_N = \hat{\beta}_0(N) - \hat{\beta}_0(N-1)$. Then, the variance of Δ_N as
shown in Appendix 2, is given by

$$Var(\Delta_N) = Var(\hat{\beta}_0(N-1)) - Var(\hat{\beta}_0(N)) \qquad (9)$$

and it can be computed using the formula for $Var(\hat{\beta}_0)$ in Eq. (3).
Statistically, the one-σ value of Δ_N is considered as the
distance which should be taken out by the interceptor after the
Nth pulse or range $r = r_a - (N-1) v_c/prf$.

12

An illustration of the engagement model is shown in Fig. 4 where the prediction error of the sensor [$\sigma(\beta_0)$, Eq. (3)], the divert capability of the interceptor [D, Eq. (4)] and the one-pulse position change [$\sigma(\Delta_N)$, Eq. (9)] are plotted as functions of the range r. At very short range, $\sigma(\Delta_N)$ is larger than $\sigma(\beta_0)$. This is because the relative change in σ_i between pulses is significant. As long as the time between pulses is much shorter than the missile response time, this effect does not influence the miss distance. The critical point where the divert and position change curves cross over each other is designated as "A". The corresponding miss distance, M, defined as the prediction error at this time is .4 meter.

Based on the above described miss distance model, sample numerical results are presented in the following. The nominal operating point of the engagement is assumed to be r_a = 5 km, v_c =5 km/s, σ_θ= 2 mr, prf = 100, τ_m= 40 ms and a = 40 g. The miss distance variations corresponding to certain excursions of σ_θ, τ_m, a, and prf are shown in Figures 5-8, respectively. Two cases are considered in each figure, uncorrelated noise and correlated noise. In the latter case, the correlation time is set equal to the missile response time, i.e. τ_c= τ_m.

Two observations are very distinct from these figures. Firstly, the miss distance increases when σ_θ becomes larger, when

13

τ_m becomes longer, when a becomes smaller or when prf becomes lower. The changes are more prominent for the case of correlated noise. Secondly, the effect of correlation degrades the achievable miss distance in all cases under consideration. The degrees of degradation vary but they are particularly significant if τ_m is large or if a is small.
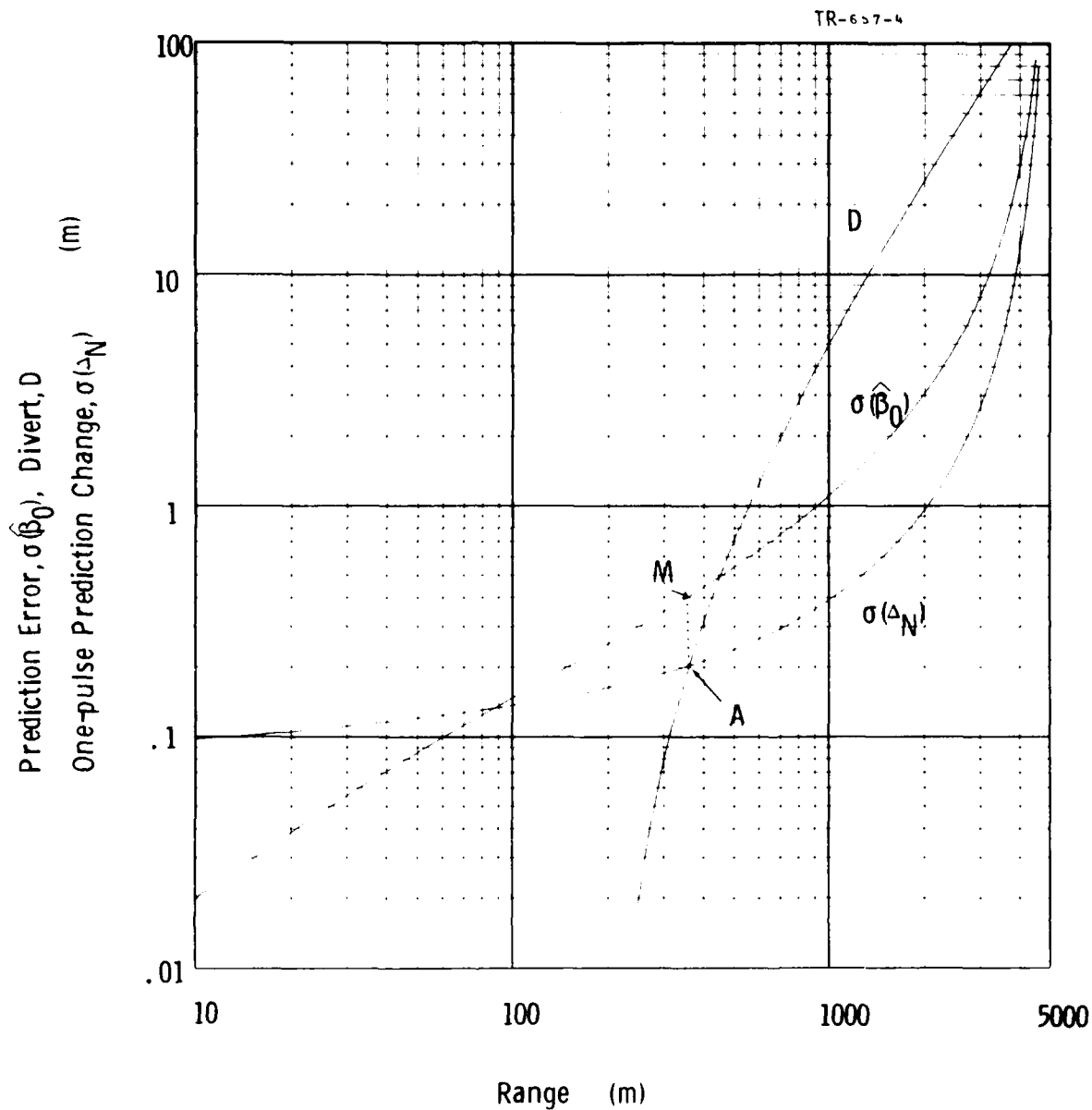
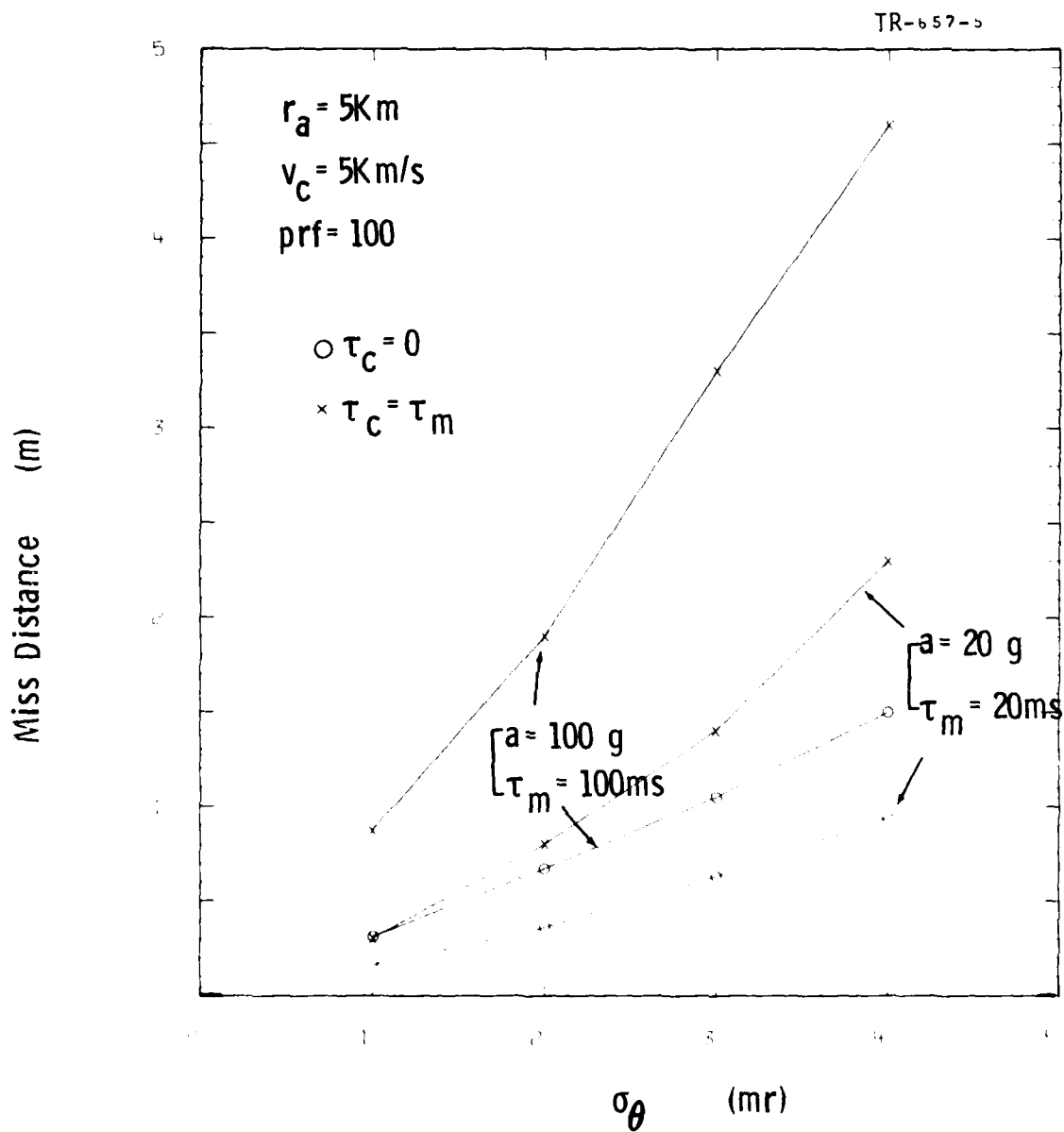Fig. 4. An illustration of the engagement model.

Fig. 5. Miss distances for various magnitudes of the radome residual error.
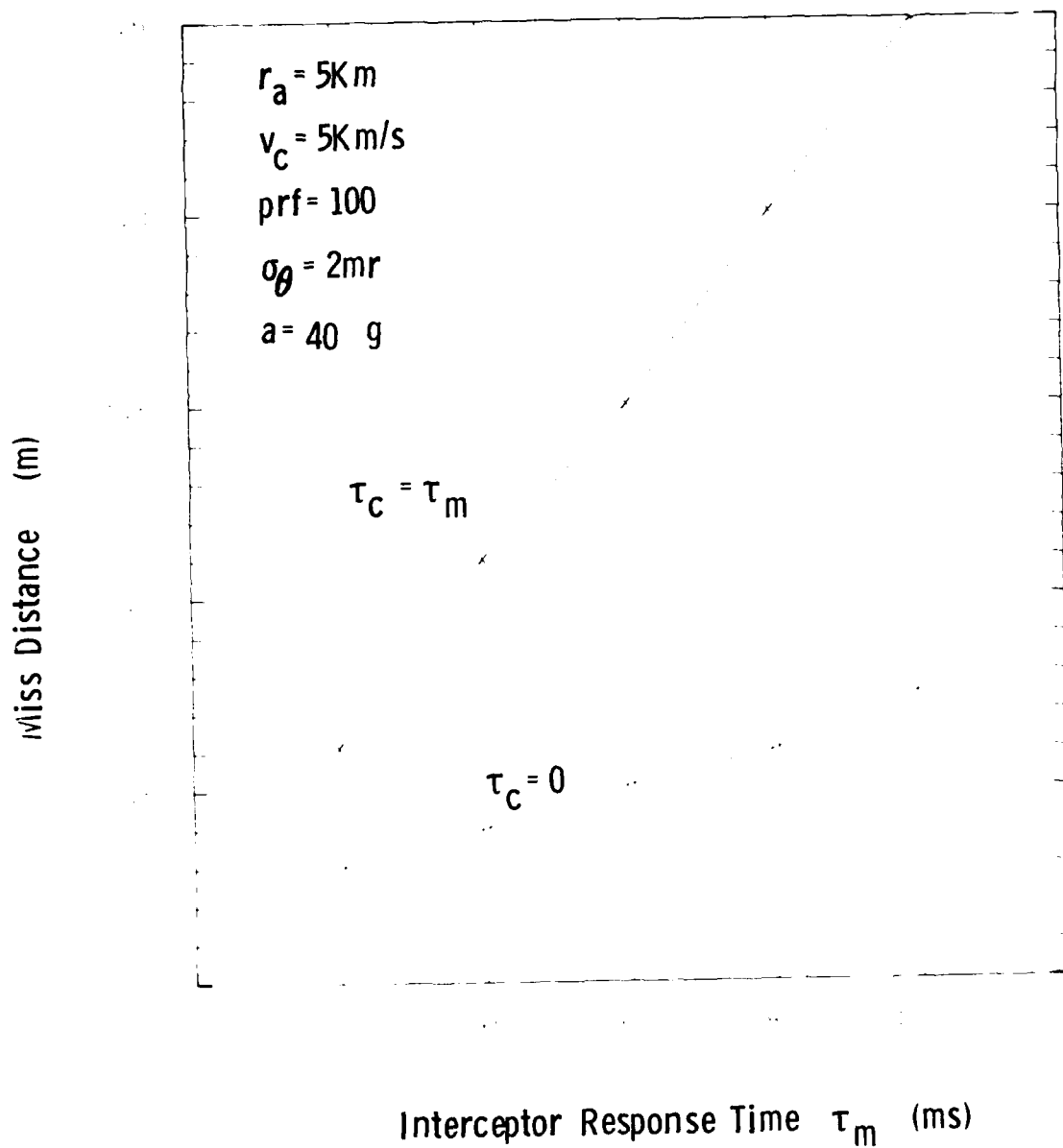
Fig. 6.   Miss distance for various interceptor response times.
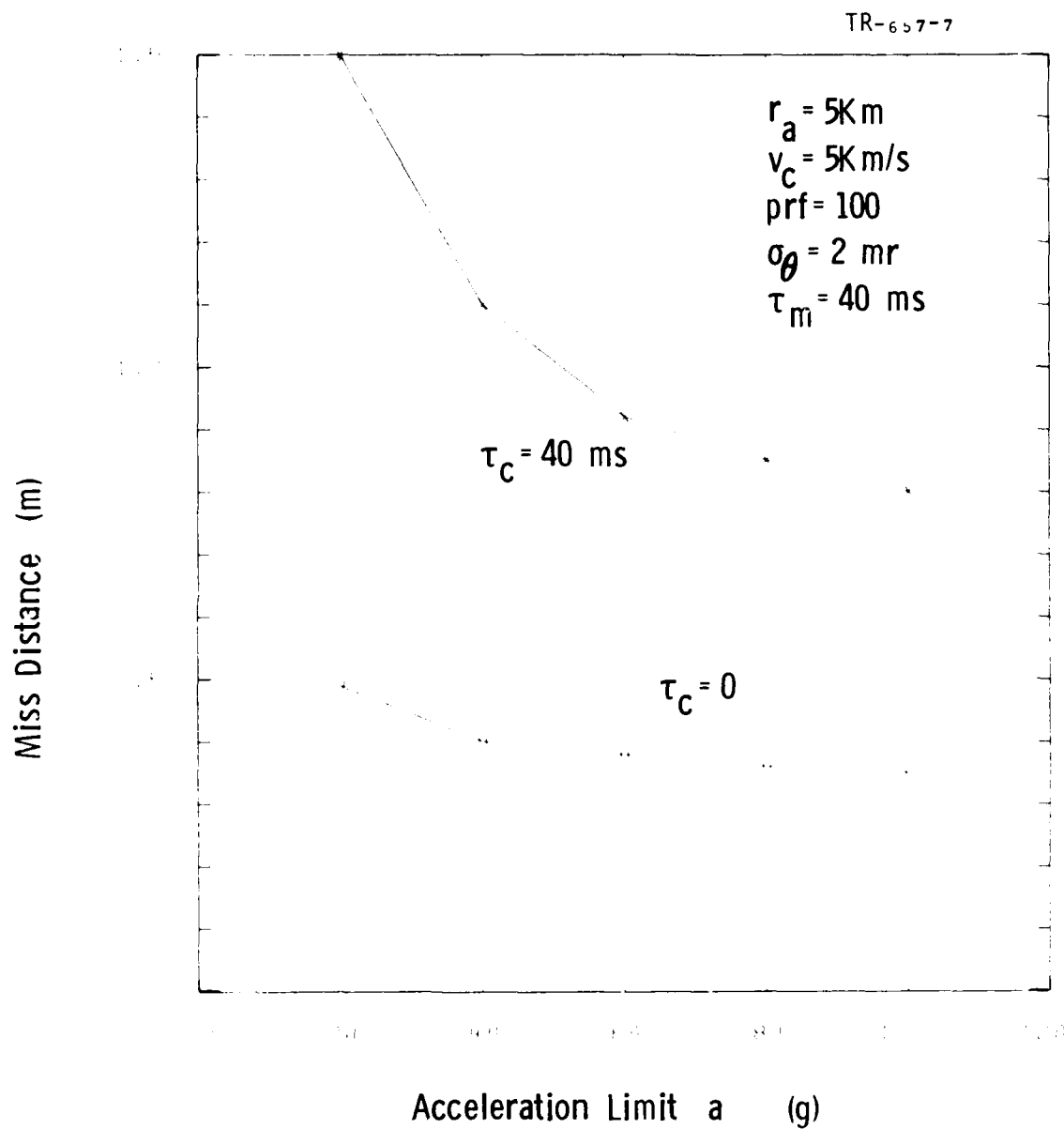
Fig. 7.   Miss distances for various interceptor acceleration limits.
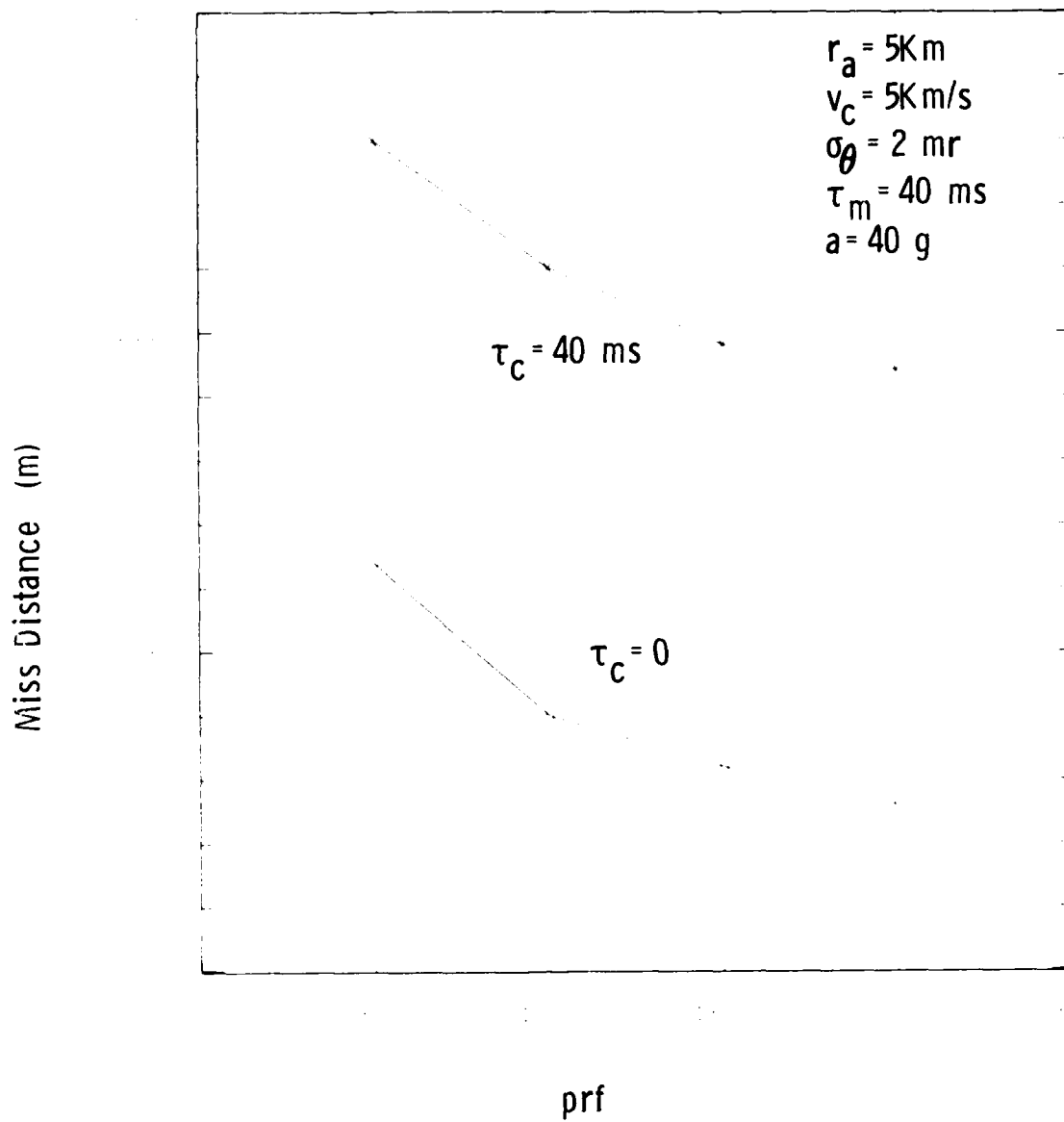
Fig. 8. Miss distances for various radar prf.

V.   CONCLUSION

We have modified the basic model of a radar homing engagement presented in [1] to include the boresight error effect and a refined miss distance model. The boresight error is treated as an exponentially correlated random noise additive to the target position measurement. The final miss distance is estimated as the prediction error at the range where the divert capability of the interceptor is just sufficient to erase the change in predicted intercept points from the previous to the current predictions. Numerical results show that the effect of correlation generally increases the achievable miss distance, particularly when the interceptor response time is large or when the acceleration limit is small. Finally, we would caution the reader that even with some modifications on the basic model, the model described in this report is still very simplified and should be used to give a lower bound on achievable miss distance.

APPENDIX A: Derivation of Prediction Error Formula

In this appendix, we will derive Eqs. (6) and (7) of Section 3. They are actually obtained as a special case of a rather general approach. Given a sequence of measurements z_i ($i=1,\ldots,N$) at r_i and a linear regression model

$$z_i = \beta_0 + \beta_1 r_i + w_i \qquad i=1,\ldots,N \qquad \text{(A1)}$$

where w_i is the corruption noise; the problem is to estimate β_0 and β_1. In vector-matrix form, (A1) can be rewritten as

$$\underline{z} = X\underline{\beta} + \underline{w} \qquad \text{(A2)}$$

where

$$\underline{z} = (z_1,\ldots,z_N)^t$$

$$\underline{w} = (w_1,\ldots,w_N)^t$$

$$\underline{\beta} = (\beta_0,\beta_1)^t \qquad \text{(A3)}$$

$$X = (\underline{j},\underline{r})$$

$$\underline{j} = (1,\ldots,1)^t$$

$$\underline{r} = (r_1,\ldots,r_N)^t$$

Let W denote the covariance matrix of the noise sequence, i.e.,

$$W = E(\underline{w}\ \underline{w}^t)$$

Then, according to the well-known Gauss-Markov theorem [6], the best linear unbiased estimate of $\underline{\beta}$, denoted by $\overset{\wedge}{\underline{\beta}}$, is given as

$$\overset{\wedge}{\underline{\beta}} = (X^t\ W^{-1}\ X)^{-1}\ X^t\ W^{-1}\ \underline{z} \qquad (A4)$$

and the covariance of $\overset{\wedge}{\underline{\beta}}$ is

$$cov(\overset{\wedge}{\underline{\beta}}) = (X^t\ W^{-1}\ X)^{-1} \qquad (A5)$$

(A4) and (A5) can be simplified if W possesses the special structure that

$$W = \begin{pmatrix} \sigma_1^2 & \sigma_1\ \sigma_2\ \rho\ \cdots\cdots\ \sigma_1\ \sigma_N\ \rho^{N-1} \\ \sigma_1\ \sigma_2\ \rho & \sigma_2^2\ \cdots\cdots\ \sigma_2\ \sigma_N\ \rho^{N-2} \\ \vdots\qquad\qquad \vdots\quad\ddots\qquad\quad \vdots \\ \sigma_1\ \sigma_N\ \rho^{N-1} & \sigma_2\ \sigma_N\ \rho^{N-2}\cdots\ \sigma_N^2 \end{pmatrix} \qquad (A6)$$

as described in Section 3. It is easy to see that W in this case can be decomposed into

$$W = D V D \tag{A7}$$

where

$$D = \text{diag} (\sigma_1, \ldots, \sigma_N) \tag{A8}$$

and

$$
V = \begin{pmatrix}
1 & & \cdots & \rho^{N-1} \\
& 1 & \cdots & \rho^{N-2} \\
\vdots & \vdots & & \vdots \\
\rho^{N-1} & \rho^{N-2} & \cdots & 1
\end{pmatrix} \tag{A9}
$$

By direct substitutions and using the fact that [7]

$$
V^{-1} = \frac{1}{1-\rho^2}
\begin{pmatrix}
1 & -\rho & & O \\
-\rho & 1+\rho^2 & & -\rho \\
& & 1+\rho^2 & \\
O & & -\rho & 1
\end{pmatrix} \tag{A10}
$$

both $\hat{\underline{\beta}}$ and $\text{cov}(\hat{\underline{\beta}})$ can be expressed explicitly without the matrix inversions. Specifically, $\hat{\beta}_0$ and $\text{var}(\hat{\beta}_0)$ are given by

23

$$\hat{\beta}_0 = \alpha \left\{ f(\underline{r}, \underline{r})\ f(\underline{z}, \underline{j}) - f(\underline{r}, \underline{z})\ f(\underline{r}, \underline{j}) \right\} \qquad \text{(A11)}$$

$$\text{var}(\hat{\beta}_0) = (1-\rho^2)\ \alpha\ f(\underline{r}, \underline{r}) \qquad \text{(A12)}$$

where

$$\alpha = \left\{ f(\underline{j}, \underline{j})\ f(\underline{r}, \underline{r}) - f^2(\underline{r}, \underline{j}) \right\}^{-1}$$

$$f(\underline{u}, \underline{v}) = \left\{ \sum_{i=1}^{N-1} \left(\frac{u_i}{\sigma_i} - \frac{\rho\ u_{i+1}}{\sigma_{i+1}} \right) \left(\frac{v_i}{\sigma_i} - \frac{\rho\ v_{i+1}}{\sigma_{i+1}} \right) \right\} + (1-\rho^2)\ \frac{u_N\ v_N}{\sigma_N^2}$$

For the case that $\sigma_i = \sigma_\theta\ r_i$ with σ_θ being a constant (A11) and (A12), reduce to (6) and (7) of Section 3.

24

APPENDIX B: Derivation of Formula for Intercept Point
              Prediction Change from Pulse-to-Pulse

In this appendix, we will derive Eq. (9) of Section 4 using the observation model described by (A2) and (A6). Two subscripts "N" and "N-1" will be used to denote quantities constructed from N and N-1 measurements, respectively. For example, $\hat{\underline{\beta}}_N$ and $\hat{\underline{\beta}}_{N-1}$ denote the estimates of $\underline{\beta}$ at the Nth pulse and the (N-1)th pulse. During the derivation, three important relationships are obtained in order: (1) cov $(\hat{\underline{\beta}}_N)$ can be computed recursively, (2) cov $(\hat{\underline{\beta}}_N, \hat{\underline{\beta}}_{N-1})$ = cov $(\hat{\underline{\beta}}_N)$ and (3) cov $(\hat{\underline{\beta}}_N - \hat{\underline{\beta}}_{N-1})$ = cov $(\hat{\underline{\beta}}_{N-1})$ - cov $(\hat{\underline{\beta}}_N)$.

From (A5), we have

$$cov(\hat{\underline{\beta}}_N) = (X_N^t \ W_N^{-1} \ X_N)^{-1} \tag{B1}$$

Both X_N and W_N^{-1} can be partitioned as follows:

$$X_N = \left(-\frac{X_{N-1}}{\underline{p}^t} - \right) \tag{B2}$$

$$W_N^{-1} = D_N^{-1} \ V_N^{-1} \ D_N^{-1}$$

$$= \begin{pmatrix} D_{N-1}^{-1} & \vdots & O \\ - - - & \vdots & - - \\ O & \vdots & \sigma_N^{-1} \end{pmatrix} \begin{pmatrix} V_{N-1}^{-1} + S & \vdots & \begin{matrix} 0 \\ \vdots \\ -\rho/(1-\rho^2) \end{matrix} \\ - - - - - & \vdots & - - - \\ 0 - - \dfrac{-\rho}{1-\rho^2} & \vdots & \dfrac{1}{1-\rho^2} \end{pmatrix} \begin{pmatrix} D_{N-1}^{-1} & \vdots & O \\ - - - & \vdots & - - \\ O & \vdots & \sigma_N^{-1} \end{pmatrix}$$

$$= \begin{pmatrix} W_{N-1}^{-1} + T & \vdots & \underline{f} \\ - - - - - & \vdots & - - \\ \underline{f}^t & \vdots & g \end{pmatrix} \tag{B3}$$

where

$$\underline{p}^t = (1, \; r_N) \tag{B4a}$$

$$S = \begin{pmatrix} 0 & & & & \\ & \ddots & & & O \\ & & 0 & \\ O & & 0 & \dfrac{\rho^2}{1-\rho^2} \end{pmatrix} \tag{B4b}$$

$$T = S \; / \; \sigma_{N-1}^2 \tag{B4c}$$

$$\underline{f}^t = (0, \ldots 0, \; \frac{-\rho}{(1-\rho^2) \; \sigma_N \; \sigma_{N-1}} \;) \tag{B4d}$$

$$g = [(1-\rho^2) \; \sigma_N^2 \;]^{-1} \tag{B4e}$$

Substituting (B2) and (B3) into (B1) and carrying out the matrix manipulation yields

$$\text{cov}(\hat{\underline{\beta}}_N) = (X_{N-1}^t \ \hat{W}_{N-1}^{-1} \ X_{N-1} + X_{N-1}^t \ T \ X_{N-1} + \underline{p} \ \underline{f}^t \ X_{N-1} +$$

$$X_{N-1}^t \ \underline{f} \ \underline{p}^t + \underline{p} \ g \ \underline{p}^t)^{-1} \tag{B5}$$

By direct matrix multiplications and summation, it can be shown that the summation of the last four terms within parentheses of (B5) is equal to

$$\frac{1}{1-\rho^2} \quad \underline{q}_N \ \underline{q}_N^t$$

where

$$\underline{q}_N = \begin{pmatrix} \dfrac{\rho}{\sigma_{N-1}} & - & \dfrac{1}{\sigma_N} \\[4mm] \dfrac{\rho \ r_{N-1}}{\sigma_{N-1}^2} & - & \dfrac{r_N}{\sigma_N} \end{pmatrix} \tag{B6}$$

Therefore

$$\text{cov}(\hat{\underline{\beta}}_N) = (X_{N-1}^t \ W_{N-1}^{-1} \ X_{N-1} + \frac{1}{1-\rho^2} \quad \underline{q}_N \ \underline{q}_N^t)^{-1}$$

$$= (X_{N-1}^t \ \hat{W}_{N-1}^{-1} \ X_{N-1})^{-1} - Q_N$$

$$= \text{cov}(\hat{\underline{\beta}}_{N-1}) - Q_N \tag{B7a}$$

where

$$Q_N = \frac{(1-\rho^2)^{-1} \; cov(\hat{\underline{\beta}}_{N-1}) \; \underline{q}_N \; \underline{q}_N^t \; cov(\hat{\underline{\beta}}_{N-1})}{1 + (1-\rho^2)^{-1} \; \underline{q}_N^t \; cov(\hat{\underline{\beta}}_{N-1}) \; \underline{q}_N} . \tag{B7b}$$

In the above, the well-known matrix inversion lemma [7] has been used.

Next, we will show that the covariance between $\hat{\underline{\beta}}_N$ and $\hat{\underline{\beta}}_{N-1}$, $cov(\hat{\underline{\beta}}_N, \hat{\underline{\beta}}_{N-1})$, is equal to $cov(\hat{\underline{\beta}}_N)$. Let

$$U_N = (X_N^t \; W_N^{-1} \; X_N)^{-1} \; X_N^t \; W_N^{-1} . \tag{B8}$$

Then the following relationships are immediate:

$$U_N = cov(\hat{\underline{\beta}}_N) \; X_N^t \; W_N^{-1}$$

$$\hat{\underline{\beta}}_N = U_N \; \underline{z}_N$$

$$U_N \; X_N = I .$$

Using these equations, we have

$$cov(\hat{\underline{\beta}}_N, \hat{\underline{\beta}}_{N-1}) \triangleq E\{(\hat{\underline{\beta}}_{N-1} - \underline{\beta})(\hat{\underline{\beta}}_N - \underline{\beta})^t\}$$

$$= E\{U_{N-1} (\underline{z}_{N-1} - X_{N-1} \; \underline{\beta})(\underline{z}_N - X_N \; \beta)^t \; U_N^t\} \tag{B9}$$

$$= U_{N-1} \; E\{\underline{w}_{N-1} \; \underline{w}_N^t\} \; U_N^t . \tag{B10}$$

It is easy to see that

$$E\{\underline{w}_{N-1} \; \underline{w}_N^t\} = (W_{N-1} \; \vdots \; \underline{h})$$

where

$$h^t = (\sigma_1 \ \sigma_N \ \rho^{N-1}, \ldots, \ \sigma_{N-1} \ \sigma_N \ \rho)$$

and, using (B2) and (B3),

$$U_N = \text{cov}(\hat{\underline{\beta}}_N) \ (X_{N-1}^t \ \vdots \ \underline{p}) \left(\begin{array}{c|c} W_{N-1}^{-1} + T & \underline{f} \\ \hline \underline{f}^t & g \end{array} \right)$$

(B11)

$$= \text{cov}(\hat{\underline{\beta}}_N) \ (X_{N-1}^t \ W_{N-1}^{-1} + X_{N-1}^t \ T + \underline{p} \ \underline{f}^t \ \bigm| \ X_{N-1}^t \ \underline{f} + \underline{p} \ g)$$

Substituting (B10) and (B11) into (B9) and carrying out the matrix manipulations, (B9) can be reduced to

$$\text{cov}(\hat{\underline{\beta}}_N, \ \hat{\underline{\beta}}_{N-1}) = \{ I + \text{cov}(\hat{\underline{\beta}}_{N-1}) \ [X_{N-1}^t (W_{N-1}^{-1} \ \underline{h} \ \underline{f}^t + T^t) \ X_{N-1}$$

$$+ X_{N-1}^t \ (W_{N-1}^{-1} \ \underline{h} \ g + \underline{f}) \ \underline{p}^t] \ \} \ \text{cov}(\hat{\underline{\beta}}_N).$$

By direct expansions, it can be shown that

$$W_{N-1}^{-1} \ \underline{h} \ \underline{f}^t = -T^t$$

and

$$W_{N-1}^{-1} \ \underline{h} \ g = -\underline{f} \ .$$

Therefore we have

$$\text{cov}(\hat{\underline{\beta}}_N, \ \hat{\underline{\beta}}_{N-1}) = \text{cov}(\hat{\underline{\beta}}_N).$$

(B12)

Now, we are ready to obtain Eq.(9) of Section 4. Since $E(\hat{\underline{\beta}}_N) = E(\hat{\underline{\beta}}_{N-1}) = \underline{\beta}$, we have

29

$$\text{cov}(\hat{\underline{\beta}}_N - \underline{\beta}_{N-1}) = E\{[(\hat{\underline{\beta}}_N - \underline{\beta}) - (\hat{\underline{\beta}}_{N-1} - \underline{\beta})] \ [(\hat{\underline{\beta}}_N - \underline{\beta}) \ (\hat{\underline{\beta}}_{N-1} - \underline{\beta})]^t\}$$

$$= \text{cov}(\hat{\underline{\beta}}_N) + \text{cov}(\hat{\underline{\beta}}_{N-1}) - 2 \ \text{cov}(\hat{\underline{\beta}}_N, \hat{\underline{\beta}}_{N-1}). \quad \text{(B13)}$$

Using (B7) and (B12), we have finally

$$\text{cov}(\hat{\underline{\beta}}_N - \hat{\underline{\beta}}_{N-1}) = \text{cov}(\hat{\underline{\beta}}_{N-1}) - \text{cov}(\hat{\underline{\beta}}_N) = Q_N. \quad \text{(B14)}$$

30

ACKNOWLEDGMENT

REFERENCES

1. S. D. Weiner, "A Simple Graphical Model for Analyzing Radar Homing Interceptor Engagement", Technical Note 1979-82, Lincoln Laboratory, M.I.T. (17 December 1979), AD-AO82460/7.

2. C. B. Chang, "A Model for Sensor-Interceptor Trade-Off Analysis", TR-599, Lincoln Laboratory, M.I.T. (18 January 1982), AD-A112046/8.

3. D. Keene and J. Potter, "Augmented Kalman Filter for Improving ENNK Radar Navigation", DWK-1-82, The Charles Stark Draper Laboratory, Inc., Cambridge, MA.

4. R. Phillips, "Radome Slope Error Model", 10-E-83-REP-002, The Charles Stark Draper Laboratory, Inc., Cambridge, MA.

5. E. Parzen, *Modern Probability and Its Applications*, (Wiley, New York, 1960).

6. Helge Toutenburg, *Prior Information in Linear Models*, (Wiley, NY, 1982).

7. F. A. Graybill, *Introduction to Matrices with Applications in Statistics* (Wadsworth, Belmont, CA, 1969).

SECURITY CLASSIFICATION OF THIS PAGE *(When Data Entered)*

REPORT DOCUMENTATION PAGE		READ INSTRUCTIONS BEFORE COMPLETING FORM
1. REPORT NUMBER ESD-TR-83-045	2. GOVT ACCESSION NO. AD·A136 108	3. RECIPIENT'S CATALOG NUMBER
4. TITLE *(and Subtitle)* A Refined Model for Radar Homing Intercepts		5. TYPE OF REPORT & PERIOD COVERED Technical Report
		6. PERFORMING ORG. REPORT NUMBER Technical Report 657
7. AUTHOR*(s)* Ming-Jer Tsai and Stephen D. Weiner		8. CONTRACT OR GRANT NUMBER*(s)* F19628-80-C-0002
9. PERFORMING ORGANIZATION NAME AND ADDRESS Lincoln Laboratory, M.I.T. P.O. Box 73 Lexington, MA 02173-0073		10. PROGRAM ELEMENT, PROJECT, TASK AREA & WORK UNIT NUMBERS Program Element Nos. 63304A and 63308A
11. CONTROLLING OFFICE NAME AND ADDRESS Ballistic Missile Defense Program Office Department of the Army 5001 Eisenhower Avenue Alexandria, VA 22333		12. REPORT DATE 27 October 1983
		13. NUMBER OF PAGES 40
14. MONITORING AGENCY NAME & ADDRESS *(if different from Controlling Office)* Electronic Systems Division Hanscom AFB, MA 01731		15. SECURITY CLASS. *(of this report)* Unclassified
		15a. DECLASSIFICATION DOWNGRADING SCHEDULE

16. DISTRIBUTION STATEMENT *(of this Report)*

Approved for public release; distribution unlimited.

17. DISTRIBUTION STATEMENT *(of the abstract entered in Block 20, if different from Report)*

18. SUPPLEMENTARY NOTES

None

19. KEY WORDS *(Continue on reverse side if necessary and identify by block number)*

radar homing intercept	radome refraction
engagement model	prediction error
sensor noise model	miss distance

20. ABSTRACT *(Continue on reverse side if necessary and identify by block number)*

In this report, we extend a simple graphical model for analyzing radar homing interceptor engagements (1) to include the radome refraction error effect and a refined miss distance estimator. The residual radome error is treated as an additive exponentially correlated noise with correlation time equal to the interceptor response time. The miss distance is estimated as the error in predicting the target cross-range position at intercept at the range where the interceptor divert capability becomes just insufficient to correct the distance difference between the previous and the current predicted intercept points. The analytical and numerical results show that the prediction error is a strong function of the correlation time and the effect of correlation generally increases the achievable miss distance especially when the interceptor response time is large.

DD FORM 1473   EDITION OF 1 NOV 65 IS OBSOLETE
1 Jan 73